Title

Observed variation in soil properties can drive large variation in modelled forest functioning and composition during tropical forest secondary succession

Journal

New Phytologist, 223(4)

ISSN

0028-646X

Authors

Medvigy, David

Wang, Gangsheng

Zhu, Qing

et al.

Publication Date

2019-09-01

DOI

10.1111/nph.15848

Peer reviewed

Observed variation in soil properties can drive large variation in modelled forest functioning and composition during tropical forest secondary succession

David Medvigy[1], Gangsheng Wang[2,3], Qing Zhu[4], William J. Riley[4], Annette M. Trierweiler[1], Bonnie G. Waring[5], Xiangtao Xu[1,6] and Jennifer S. Powers[7]

[1] Department of Biological Sciences, University of Notre Dame, Notre Dame, IN 46556, USA; [2] Institute for Environmental Genomics and Department of Microbiology & Plant Biology, University of Oklahoma, Norman, OK 73019, USA; [3] Climate Change Science Institute and Environmental Sciences Division, Oak Ridge National Laboratory, Oak Ridge, TN 37831, USA; [4] Climate and Ecosystem Sciences Division, Earth Sciences Division, Lawrence Berkeley National Laboratory, Berkeley, CA 94720, USA; [5] Biology Department and Ecology Center, Utah State University, Logan, UT 84322, USA; [6] Department of Organismic and Evolutionary Biology, Harvard University, Cambridge, MA 02138, USA; [7] Department of Ecology, Evolution, and Behavior, University of Minnesota, St Paul, MN 55108, USA

Correspondence: Email: dmedvigy@nd.edu

Summary

Censuses of tropical forest plots reveal large variation in biomass and plant composition. This paper evaluates whether such variation can emerge solely from realistic variation in a set of commonly measured soil chemical and physical properties.

Controlled simulations were performed using a mechanistic model that includes forest dynamics, microbe-mediated biogeochemistry, and competition for nitrogen and phosphorus. Observations from 18 forest inventory plots in Guanacaste, Costa Rica were used to determine realistic variation in soil properties.

In simulations of secondary succession, the across-plot range in plant biomass reached 30% of the mean and was attributable primarily to nutrient limitation and secondarily to soil texture differences that affected water availability. The contributions of different plant functional types to total biomass varied widely across plots and depended on soil nutrient status. In Central America, soil-induced variation in plant biomass increased with mean annual precipitation because of changes in nutrient limitation.

In Central America, large variation in plant biomass and ecosystem composition arises mechanistically from realistic variation in soil properties. The degree of biomass and compositional variation is climate sensitive. In general, model predictions can be improved through better representation of soil nutrient processes, including their spatial variation.

Introduction

Seventy years ago, Leslie Holdridge divided the Earth's land areas into bioclimatic classes or ‘life zones’ based on water and energy considerations (Holdridge, 1947). While undoubtedly a useful concept, bioclimatic classifications treat terrestrial ecosystems as homogeneous on scales over which climate is approximately constant. This scale, from this point forward the ‘regional’ scale, can operationally be defined as the size of a few climate model grid cells (*c*. 100s of km). For practical purposes, homogeneity on regional scales has also been assumed by some techniques used to analyse observational data. For example, carbon dioxide (CO_2) flux maps do not account for fine-scale environmental variability and therefore exhibit little subregional-scale variability (Beer *et al*., 2010). Similarly, tropical vegetation biomass and CO_2 fluxes simulated by mechanistic ecosystem models tend to be homogeneous on regional scales because these models are rarely driven by fine-scale environmental variation (Sitch *et al*., 2003, 2015; Levy *et al*., 2004; Thornton *et al*., 2007).

Ecological theory has long held that variability in ‘state factors’ (soil parent material, relief, time, potential vegetation, climate) (Jenny, 1941) should support subregional spatial variation in ecosystem functioning. In tropical ecosystems, observations have identified substantial subregional-scale variation in biogeochemical functioning (Townsend *et al*., 2008), above-ground biomass (Jubanski *et al*., 2013; Avitabile *et al*., 2016), and plant nutrient limitation (Augusto *et al*., 2017). Although, the mechanisms by which fine-scale environmental variation might affect regional-scale averages in the tropics are not yet well understood, the effects are known to be large in other ecosystems (Pappas *et al*., 2015).

Here, we evaluate whether realistic subregional-scale variation in soil properties can lead to large variation in ecosystem model simulations. While there is a two-way interaction between plants and soils (Binkley & Giardina, 1998; Waring *et al*., 2015a; Fujii *et al*., 2017), we are here focused on geologically inherited soil properties. Soil geology and parent material are typically heterogeneous on subregional scales, with this heterogeneity having been dubbed ‘geodiversity’ (Gray, 2008; Ruban, 2010). Steep gradients of topography, soil weathering status, and dust deposition over relatively small spatial scales can amplify local biogeochemical and hydrological heterogeneity in tropical forests (Townsend *et al*., 2008). This site-level variation in soils has been empirically linked to variation in vegetation. For example, soils in Neotropical forests are strong predictors of species distributions (Clark *et al*., 1998; John *et al*., 2007; Fayolle *et al*., 2012; Condit *et al*., 2013; Figueiredo *et al*., 2018; Werden *et al*., 2018) and variation in soil parent material globally has been linked to differences in phosphorus (P) limitation of plant productivity (Augusto *et al*., 2017). By contrast, dynamic vegetation models have typically represented only a few aspects of geodiversity (especially soil texture), and have rarely explored how geodiversity on subregional scales affects model outcomes.

To address this problem, we have developed a novel coupled model that brings together several characteristics from existing models. First, we simulate vegetation dynamics using the vegetation demographic model ED2, a model that has previously performed well in tropical forests (Levine *et al*., 2016; Xu *et al*., 2016; Longo *et al*., 2018). Second, we account for P limitation of vegetation productivity (Goll *et al*., 2012; Yang *et al*., 2014; Wang *et al*., 2015b; Q. Zhu *et al*., unpublished). The importance of P limitation is underscored by the sensitivity of plant nutrient limitation to soil parent material (Cleveland *et al*., 2011; Augusto *et al*., 2017). Third, we explicitly simulate microbial and enzyme processes because these processes can be essential for capturing ecosystem responses to environmental change (Allison *et al*., 2010; Wieder *et al*., 2015; Georgiou *et al*., 2017; Camenzind *et al*., 2018). For example, explicit representation of microbes facilitates the modelling of time-varying microbial community stoichiometry and other processes that can only be implicit in a first-order decomposition model (Tang & Riley, 2015). We also explicitly simulate enzyme dynamics. Enzymes catalyse the conversion of polymers to plant- and microbe-available monomers, with different enzymes targeting different elements. Fourth, we mechanistically simulate plant−microbe competition for nutrients (Zhu *et al*., 2016, 2017). This competition is driven in part by the concentrations of plant and microbe nutrient transporter enzymes. Our mechanistic approach is distinct from both the common relative demand (Thornton & Rosenbloom, 2005) and microbes-satisfied-first (Gerber *et al*., 2010) assumptions.

In this study, we apply our coupled model to a tropical dry forest (TDF) site in Costa Rica and regionally throughout Central America, where TDFs are common. TDFs have been observed to have large variability in both soils and vegetation (Powers *et al*., 2009; Balvanera *et al*., 2011; Powers & Perez-Aviles, 2013; Waring *et al*., 2016). Across TDFs, total soil P varies over 100-fold and plant species and their functional traits such as foliar P sort strongly over soil P gradients (Becknell & Powers, 2014). The degree of both plant P and plant nitrogen (N)-limitation varies on regional scales (Campo, 2016). Both mature (Becknell *et al*., 2012) and recovering (Poorter *et al*., 2016) TDFs exhibit strong spatial variation in above-ground biomass (AGB), and AGB variation has previously been statistically correlated with soil properties (Becknell & Powers, 2014).

We tested three hypotheses in the context of model simulations. First, variation in soil chemical and physical properties will lead to large, sustained variation, rather than transient variation, in plant biomass during secondary succession (H1). Second, because plant functional types (PFT) have different nutrient requirements and different modes of nutrient acquisition, variation in soil nutrient availability will lead to variation in PFT composition, even at the level of presence/absence (H2). Third, there will be a soil fertility−climate interactive effect on biomass and functional group composition (H3). Specifically, biomass will be more sensitive to soil fertility at high-precipitation sites than at low-precipitation sites because wetter sites are

more likely to be limited by geologically related variables such as P than by climate-related variables like precipitation. Similarly, soil fertility variation will lead to more variation in PFT composition at high-rainfall sites, where water limitation is minimal, than at low-rainfall sites.

Materials and Methods

Field sites, soil properties, and climate

We carried out grid cell-level and regional analyses. Grid cell-level analysis focused on Guanacaste, Costa Rica (Supporting Information Fig. S1) due to the availability of detailed soil and vegetation information from 18 well characterised plots in Sector Santa Rosa of Guanacaste Conservation Area and Parque Nacional Palo Verde of Arenal-Tempisque Conservation Area (Powers *et al*., 2009). All 18 plots fall within 100 km of each other, a spatial scale that is comparable to the resolution of climate models. The mean annual temperature at both Santa Rosa and Palo Verde is 25°C. Observed mean annual precipitation (MAP) varies slightly over this grid cell, with the 1980–2017 average near Santa Rosa being 1708 mm (https://www.acguanacaste.ac.cr/investigacion/datos-meterologicos) and the 2008–2017 average near Palo Verde being 1690 mm (https://tropicalstudies.org/meteoro/default.php?pestacion=1).

Soils in this region are Inceptisols with some Vertisols (Soil Survey Staff, 1999). They are developed from diverse parent materials including volcanic ignimbrite and basalt at Santa Rosa, and limestone and colluvium at Palo Verde (Hartshorn, 1983; Leiva *et al*., 2009). Sites also have varied disturbance histories. Like most TDFs (Miles *et al*., 2006), these plots are undergoing secondary forest succession and have ages ranging from 5 to 60 yr (median = 19.5). Measured soil properties are listed in Table S1. Across the 18 plots, total P varies from 31 to 1272 ppm, and per cent clay varies from 17% to 36%. They present a two-fold gradient in total soil N (from 0.21 to 0.55%). N and P seem to exert independent effects on plant community structure (Waring *et al*., 2015b). Sand content, % C, and C : N ratio also vary widely across plots. Trees in these sites have been censused annually since 2007 and biomass has been estimated (Becknell & Powers, 2014).

Our regional-scale analysis focused on Central America, but also included southern Mexico, parts of northwestern South America, and several Caribbean islands (Fig. S1). This region was selected because it includes most of the northern hemisphere Neotropical dry forests. The availability of soil and climate data throughout this region is not uniform. Gridded products for some climate and soil variables exist (for example from the World Data Centre for Soils), typically at the 50–200 km scale. However, this scale again is typical of a climate model grid box and often does not fully account for subregional-scale heterogeneity.

Model description

We coupled three models: ED2, MEND and N-COM. All of these models have individually been evaluated in tropical forests (Xu *et al*., 2016; Zhu *et al*., 2016; Wang *et al*., 2019). We briefly describe the models here. Further details are provided in Methods S1. The model code is provided in Methods S2.

ED2 is a vegetation demographic model (VDM) that simulates the growth, mortality, and recruitment of tree cohorts (Medvigy *et al*., 2009). Cohorts are characterised by their PFT, size and stem number density. Cohort size is a vector quantity and includes leaf carbon (C), wood C, fine root C and non-structural C. Plant height and diameter at breast height are allometrically related to wood C. Competition for light and water follows previous model versions and is described in Methods S1.

ED2 has previously been evaluated at the relatively nutrient-rich Palo Verde site under the assumption of no nutrient limitation (Xu *et al*., 2016) and that version of the model formed the starting point for this analysis. Here, we present a new concept of plant nutrient dynamics in ED2 (for details, see Methods S1). In our nutrient-enabled model, each cohort has non-structural C, N and P pools that do not have fixed stoichiometry. When C, N and P are initially acquired, they accumulate in the non-structural pools. The model deploys these resources to construct structural tissue (leaves, fine roots and wood) according to the same allocation rules developed for previous model versions (Medvigy *et al*., 2009). Each type of structural tissue has a fixed stoichiometry (Table S2), and therefore structural growth can be limited by either C, N or P. Before litterfall, retranslocation transfers fixed fractions of C, N and P from structural pools to non-structural pools. The C, N and P non-structural pools have maximum sizes that are set equal to twice the amount of C, N, and P, respectively, contained in a full canopy of foliage. Any C that builds up in excess is immediately subject to waste respiration, and excess N and P are released to the soil.

We have also developed plant strategies for mitigating resource limitation. Our previously published version of the model (Xu *et al*., 2016) included four TDF PFTs which spanned a range of conservative to acquisitive traits, listed in Table S2. None of these PFTs is a nitrogen fixer. Because nitrogen-fixing legume trees figure prominently in these forests (Powers *et al*., 2009; Gei *et al*., 2018), we created four new nitrogen-fixing PFTs. These fixer PFTs are parameterised exactly the same as the original four PFTs, except that they may fix nitrogen (J. H. Levy-Varon *et al*., unpublished). Depending on a fixer cohort's N economy, it can upregulate or downregulate fixation and pay a carbon cost associated with the metabolism and nodule maintenance of fixation (Gutschick, 1981). While fixation augments soil-available N, the fixer still can become N-limited as the total amount of N acquired by the plant is constrained by a maximum rate of fixation (Table S2). Finally, we allowed cohorts to increase allocation to fine roots when they are C-limited and have relatively low water potentials, indicative of water limitation (Methods S1). Cohorts do not increase their fine roots when they are nutrient limited

because, in preliminary simulations, the nutrient cost of building fine roots exceeded the nutrient benefit of the additional roots as the soil nutrient supply was exhausted. This parameterisation is also consistent with a recent TDF nutrient fertilisation experiment in Costa Rica that reported increases in fine roots in response to P fertilisation (Waring *et al*., in press).

Although ED2 (and its predecessor, ecosystem demography (ED)) have long contained a simple representation of soil N biogeochemistry (Moorcroft *et al*., 2001), the model's soil nutrient cycling has not received much evaluation and has even been deactivated in many previously published studies. There is no published version of ED2 that includes P dynamics. Rather than develop and test an entirely new soil biogeochemistry model for N and P cycling, we coupled an existing biogeochemical model with explicit microbial mechanisms of soil organic matter (SOM) decomposition (that is enzymatic catalysis) to ED2. This model, MEND (Wang *et al*., 2013, 2015a) was selected because all MEND state variables correspond to physicochemically or biologically distinguishable entities and the multiple SOM pools are measurable; it is relatively simple but accounts for key abiotic and biotic factors; it has been evaluated in subtropical and tropical forests (Wang *et al*., 2017, 2019); it contains explicit microbial and enzyme pools; and it can represent soil N and P dynamics (for details, see Methods S1).

Nutrient competition between plants, microbes, and soil surfaces was simulated using the mechanistically based N-COM model (Zhu *et al*., 2016) (see Methods S1). N-COM determines the partitioning of multiple resources (nitrate, ammonium, phosphate) between multiple substrates (plant and microbe carrier enzymes and soil mineral surfaces) (Zhu *et al*., 2016, 2017) using the Equilibrium Chemistry Approximation (Tang & Riley, 2013). Parameter values for MEND and N-COM are the previously published default values and are given in Table S3.

Simulations

We ran thousands of simulations that varied in soil properties, external nutrient input (deposition and fertilisation rates), model parameter values via sensitivity analysis, and climate forcing. These simulations are described in this section and summarised in Table S4.

Our ‘primary’ set of 18 simulations was designed to identify the effects of soil properties on ecosystem functioning and composition (Hypothesis 1). Each of these 18 simulations was initialised with the observed soil state (OSS) in one of the 18 Guanacaste inventory plots (Powers *et al*., 2009). The OSS consisted of bulk density, % sand, % clay, % C, C : N ratio, total P and extractable P (Table S1). Details of how these data are used to initialise the model are given in Methods S3. The bulk density and soil texture were held constant throughout each simulation, while other soil variables, including nutrient concentrations, were variables updated by ED2-MEND-NCOM. In this version of the model, soil texture affected soil hydrology and thermal

conductivity only, although we recognise that soil texture can also affect soil surface adsorption capacity.

Several configurations were the same in all simulations. The initial vegetation always consisted of an initial stem density of 1000 stems ha^{-1} with a height of 2 m for all PFTs. Although this initial condition is undoubtedly a simplification, it was adopted because the vegetation condition at the times of agricultural abandonment was not known. It is likely that different plots were affected differently by seed dispersal, small-scale disturbances, and the existence of remnant trees (Powers *et al*., 2009). These primary simulations were run for 35 yr to reflect a typical time since agricultural abandonment in this area (Calvo-Alvarado *et al*., 2009). This time scale is shorter than the time required for simulated vegetation and soils to equilibrate and so many model variables, including plant biomass, were expected to exhibit transient behaviour. Given our soil and climate initial conditions, it is more appropriate to think of these simulations as secondary succession that would follow a near-complete harvest of the current-day plots, rather than secondary succession that actually ensued (and which we cannot reconstruct due to lack of observed conditions at the times of abandonment). Simulations were forced with contemporary gridded climate data from 2000 to 2012 (Sheffield *et al*., 2006). This date range intentionally avoids some strong anomalies, including the unusually short wet season in 2014 and the exceptional El Niño-related drought in 2015 (O'Brien *et al*., 2018). We repeatedly recycled the 2000–2012 data to obtain a 35-yr meteorological record. Although the simulation design was more geared toward our mechanistic hypothesis testing than prediction, we compared simulated and observed biomass as a reality-check.

We also assessed model nonlinearities expected from Jensen's inequality, that is whether the average of a function is equal to the function of the average (Ruel & Ayres, 1999). Results from the 18 primary simulations were averaged, and then compared with results from a single simulation for which the initial soil state was the average of the 18 OSS (Table S4).

To quantify the effects of variation in soil nutrient status vs variation in soil texture (via its effects on hydrology), we modified our primary set of simulations to represent a nutrient fertilisation experiment. We refer to these fertilisation simulations as our '+NP' simulations (Table S4). N deposition was set to 125 kg N ha^{-1} yr^{-1} and P deposition was set to 50 kg P ha^{-1} yr^{-1}. This level of fertilisation is the same as that being used in an ongoing experiment in Guanacaste (Waring *et al*., in press) and elsewhere in the tropics (Wright *et al*., 2011). Observed site-level rates of atmospheric N deposition (*c*. 2.2 kg N ha^{-1} yr^{-1}; M. Gei, unpublished) are comparatively small. Comparison of these +NP simulations to the primary simulations allowed us to attribute differences in biomass (Hypothesis 1) and composition (Hypothesis 2) to nutrient limitation.

We carried out additional simulations to evaluate the sensitivity of model results to variation in several parameters (Methods S3). Parameters were selected for sensitivity analysis that have been associated with key processes (Reed *et al*., 2015), and/or because their sensitivity had not previously been evaluated in ED2, MEND or N-COM. Motivated by simplicity and the limited information about parameter correlations, we carried out a one-parameter-at-a-time sensitivity analysis (Murphy *et al*., 2004). Sensitivity analysis was carried out for both our primary and +NP simulations (Table S4).

The parameters that were varied were the constant rate of P release due to physical and chemical weathering, the maximum rate of phosphatase activity, plant nutrient carrier enzyme abundance relative to fine root biomass, microbial nutrient carrier enzyme abundance relative to microbial biomass, the soluble P leaching proportion (proportion of soluble P lost per proportion of soil water leached), and the dissolved organic matter (DOM) leaching proportion (proportion of DOM lost per proportion of soil water leached). Note that DOM includes dissolved organic C, N and P. Baseline values of these parameters and parameter ranges are given in Methods S3.

To evaluate the effect of background climate and therefore test Hypothesis 3, we carried out regional primary and regional +NP simulations over the domain shown in Fig. S1. Simulations were carried out at the 1° scale, consistent with the gridded climate forcing (Sheffield *et al*., 2006). The 18 regional primary simulations corresponded to each of the 18 OSS of the primary simulation set; that is each of the 18 simulations assumed one homogenous value of OSS across the region. We then conducted an additional 18 simulations for our regional +NP treatment. For these regional primary simulations (Table S4), we did not use soil information specific to each grid cell because extensive plot-level soil measurements at < 1° scale were not available throughout our domain. The grid cells therefore differed only in terms of climate forcing, which simplifies the interpretation of the results with respect to H3. We do not interpret the results as regional predictions; predictions would require simulations with the location-specific soil properties.

We carried out several other regional-scale simulations to probe the sensitivity to our assumptions about soil texture and nitrogen fixation (Methods S3).

Analysis

Estimation of biomass (above ground plus below ground) at the ecosystem or PFT level was direct: the biomass of either all cohorts (ecosystem-level biomass) or all cohorts of the same PFT (PFT-level biomass) was summed. To quantify variation over the 18 OSS, we used the biomass range (maximum minus minimum). We did not use percentiles because it was unknown to what degree any individual plot corresponded to conditions on the landscape as a whole; that is whether a particular plot corresponded to 50%, 1%, or

1/18th of the landscape. We similarly reported other aspects of forest functioning: gross primary production (GPP), microbial biomass, microbial respiration, and NH_4, NO_3, and soluble P concentrations. Because these quantities vary on a wide range of time scales, we averaged them over the final 5 yr of our primary simulations and compared results across OSS.

In our regional-scale analysis, we computed the biomass mean and range across the 18 OSS. However, we expressed the biomass range as a percentage of the mean because climate drives spatial variation in biomass even in the absence of variation due to OSS.

We also assessed variation in ecosystem composition over the 18 OSS. Here, 'composition' refers to the proportion of biomass (not stems) in each PFT. We have adopted two approaches to evaluating compositional differences. First, we computed the variance in the biomass proportion across the 18 OSS, for each model PFT. This variance has the advantage of being relatively simple to interpret: a larger variance might suggest stronger filtering by the soils. Second, we computed an entropy index (Methods S3). Large values of the entropy index indicate that a PFT does not 'prefer' particular OSS; small values of the entropy index indicate that the soils strongly filter the PFT.

Results

Observed and simulated biomass

We compared plant biomass from our primary simulations to the biomass observed at the 18 plots in 2008. For consistency, we extracted the time point for each simulated plot that corresponded to the actual plot age in 2008. We omitted two plots which had ages older than the simulation length of 35 yr. In both the observations and the model, biomass was strongly sensitive to stand age (Fig. 1). Although the simulated biomass was mostly within the range of the observations, it was nevertheless biased low. The observations also showed more scatter than the simulations. After accounting for stand age, we found no significant correlation between biomass and soil properties in the simulations (Fig. S2; Notes S1).

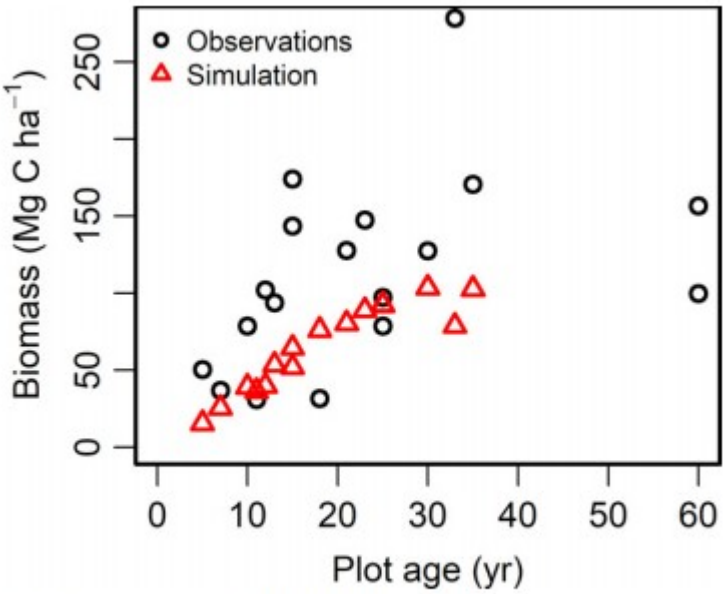

Fig. 1 Comparison of simulated and observed plant biomass across the Guanacaste plots.

Local-scale variation in the primary simulations

In our 18 primary simulations, the simulated biomass C increased from its initial condition of nearly zero to 100 Mg C ha^{-1} at 35 yr (averaged across 18 OSS), but with large variation (Fig. 2a). The biomass range (defined as the largest biomass accumulation across all OSS minus the smallest biomass accumulation) increased rapidly over the first two simulated decades and then stabilised at *c*. 30 Mg C ha^{-1} (Fig. 2c), 30% of the mean. This result supports H1. The biomass from the single simulation initialised with the average OSS was 104.1 Mg C ha^{-1} at 35 yr, 4% larger than the average of the 18 primary simulations, reflecting Jensen's inequality.

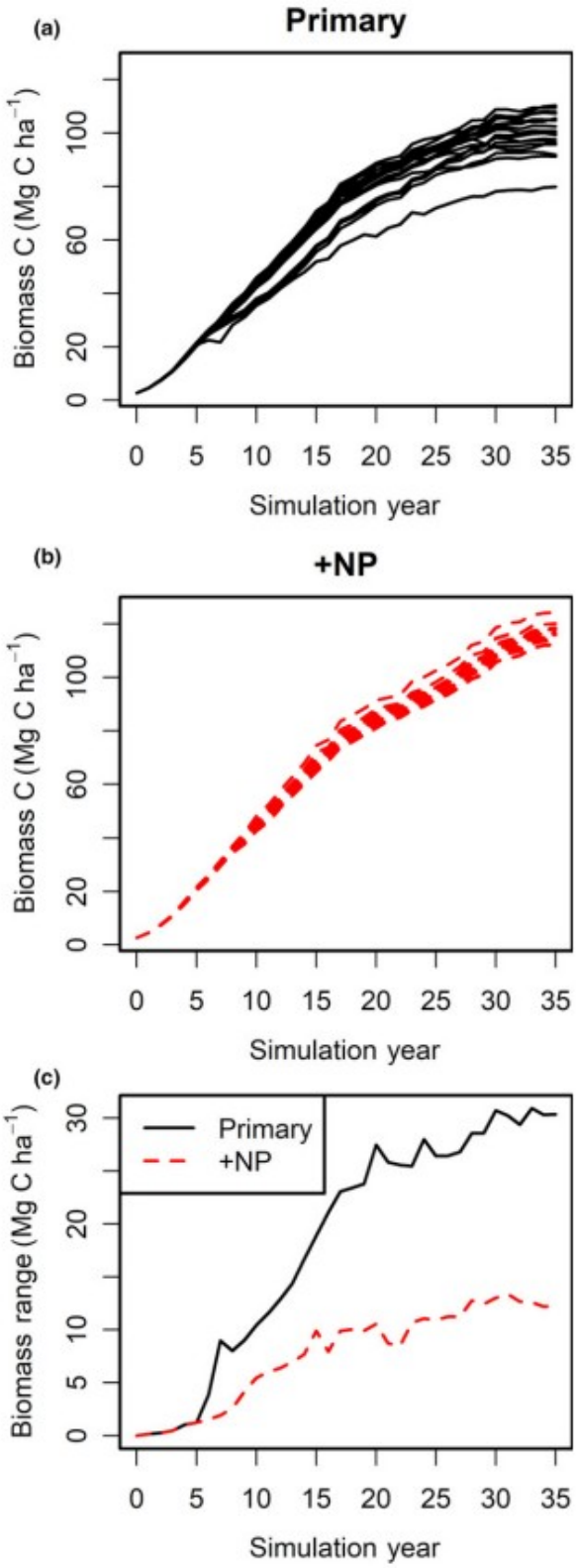

Fig. 2 Plant biomass simulated with baseline parameter values. (a) Primary simulations for the 18 observed soil states (OSS). (b) Fertilised (+NP) simulations for the 18 OSS. (c) Biomass range, defined as the maximum biomass minus the minimum biomass at each time.

The magnitude of plant biomass variation was similar to the variation in GPP, microbial biomass, and microbial respiration (Table 1). However, plant-available nutrient pools exhibited larger variability across OSS.

Table 1 Simulated variation (maximum minus minimum, divided by the mean) across observed soil states

Simulation	Plant biomass	Gross primary production	Microbial biomass	Microbial respiration	NH_4	NO_3	Soluble P
Primary	0.30	0.41	0.39	0.50	1.90	3.03	1.01
+NP	0.10	0.06	0.08	0.06	0.09	0.32	0.12

How much of the plant biomass variability across soils was due to the hydrological effects of soil texture vs soil nutrient status? In +NP simulations with baseline parameter values, plants maintained sufficiently small C : N and C : P ratios such that construction of new tissue was not nutrient limited (Fig. S3). These simulations had a median biomass of 116 Mg C ha^{-1} and a range of *c*. 12 Mg C ha^{-1} at 35 yr (Fig. 2b). Therefore, the +NP simulations had a larger median and much smaller range than the primary simulations (Fig. 2c). Similarly, variation in GPP, microbial biomass, microbial respiration, NH_4, NO_3 and soluble P were also reduced (Table 1).

Variation in the OSS affected PFT diversity in our primary simulations (H2). We considered only three of the model's PFTs because these three constituted > 95% of the observed biomass (averaged across OSS). Roughly, these PFTs corresponded to a conservative fixer, an acquisitive non-fixer, and an acquisitive fixer (PFTs 2, 5 and 6, respectively, in Table S2). Substantial variability across OSS was evident in the biomass of each of these PFTs in the primary simulations (Fig. 3a–c), with proportions varying from 0% to 60%. Less variability was evident in the +NP simulations (Fig. 3d–f).

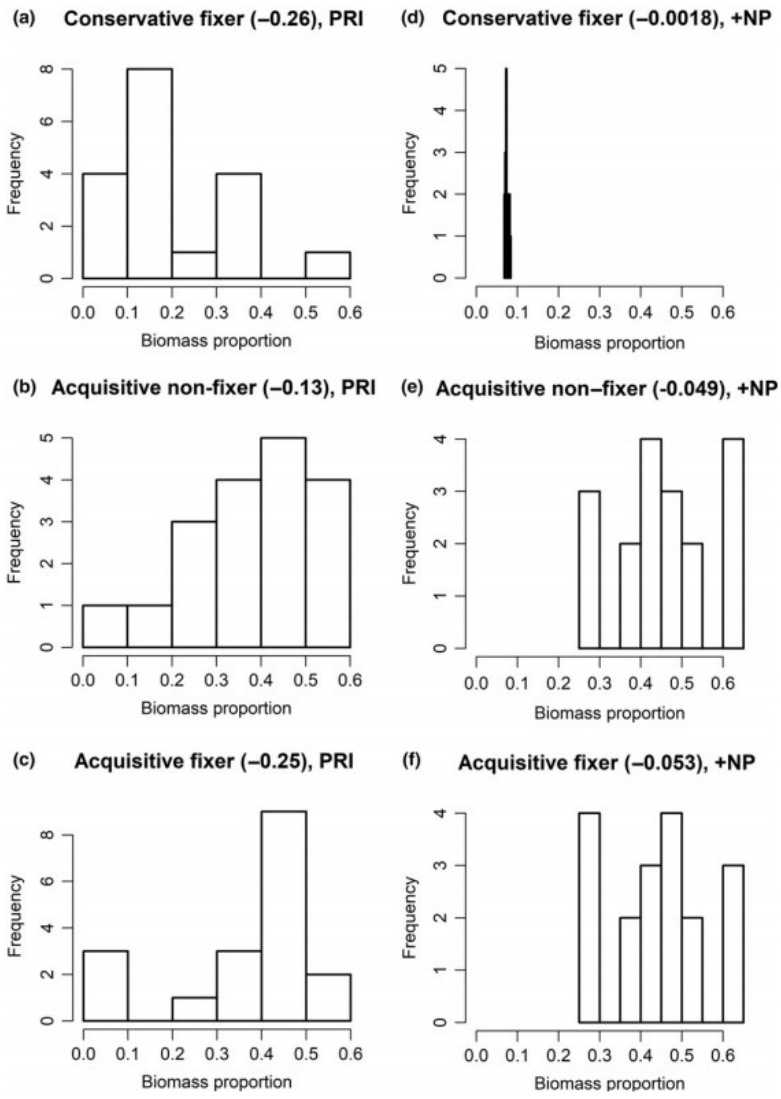

Fig. 3 The biomass proportion of particular plant functional types (PFTs) in each of the 18 observed soil states in the Guanacaste grid cell. Results are for primary (left, 'PRI') and fertilised (right, '+NP') simulations with baseline parameter values. PFTs include (a, d) a conservative fixer, (b, e) an acquisitive non-fixer, and (c, f) an acquisitive fixer. The numbers in parentheses in the plot titles are PFT-specific relative entropies derived from Eqn S16 (Supporting Information Methods S3)

Sensitivity analysis

We assessed the sensitivity of accumulated biomass at 35 yr to model parameter values. The median biomass across soil types was highly sensitive to the DOM leaching proportion (Fig. 4a): simulations with a large DOM leaching proportion accumulated over an order of magnitude less biomass than simulations where DOM leaching was small or absent. The effect of soluble P leaching proportion was qualitatively similar, but quantitatively smaller (Fig. 4b). Sufficiently low values of the plant enzyme-to-fine root ratio led to a near-collapse of plant biomass; as this variable increased, plant biomass approached a maximum of *c*. 115 Mg C ha^{-1} (Fig. 4c). The reverse occurred when the microbial enzyme-to-microbial biomass ratio was varied: for low values of this parameter, plant biomass was relatively large, but high values of this parameter led to a near-collapse of plant biomass (Fig. 4d). By contrast, plant biomass was less sensitive to either the weathering rate (Fig.

4e) or the maximum rate of phosphatase activity (Fig. 4f); the model showed only slight plant biomass increases with increasing values of these parameters. Regardless of parameterisation, the range in predicted biomass was typically either comparable to, or larger than, the range associated with our baseline parameter set.

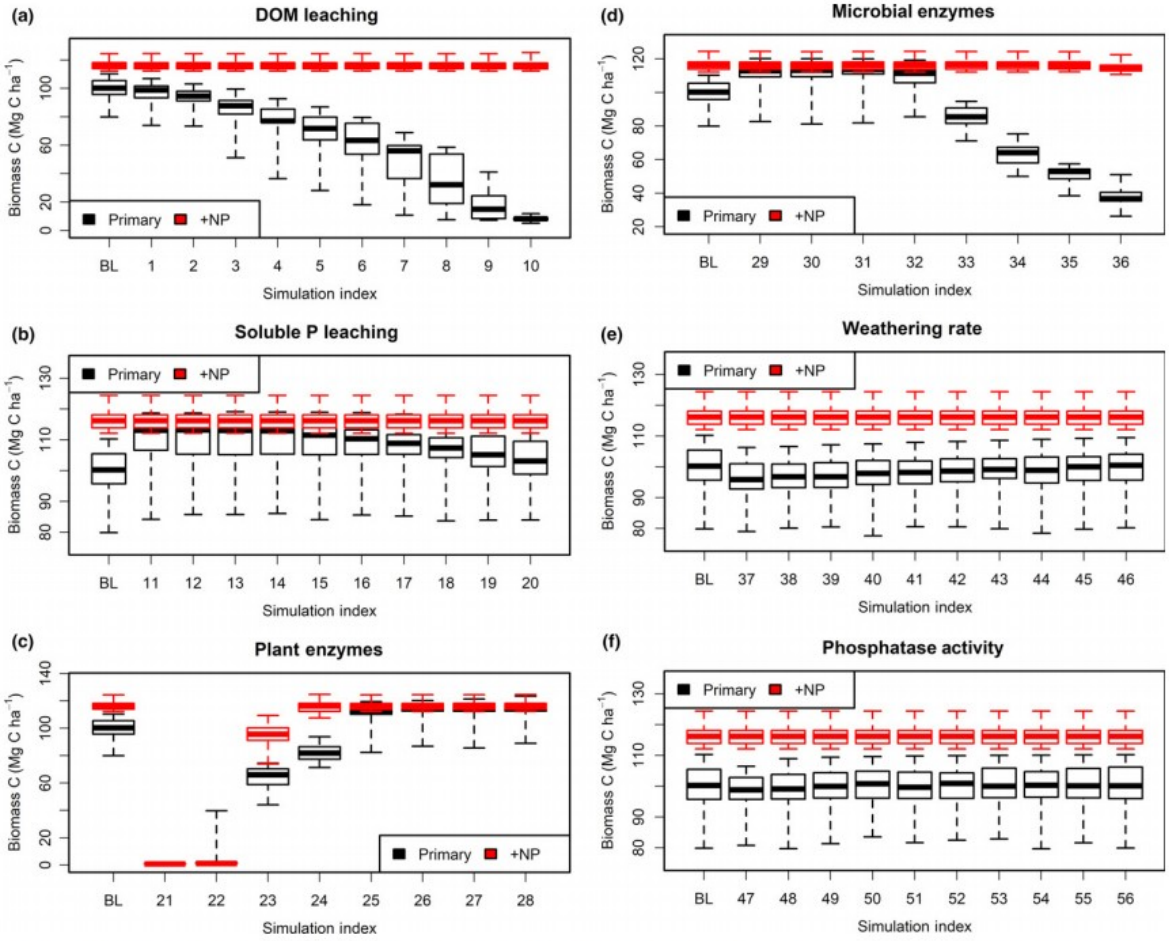

Fig. 4 Sensitivity of plant biomass at 35 yr to model parameters, for both primary (black) and fertilised ('+NP'; red) simulations. For each parameter set, the bold horizontal line denotes the median value, the box denotes the 25% and 75% quantiles, and the whiskers denote the full biomass range across observed soil states. Individual panels show sensitivity to (a) dissolved organic matter (DOM) leaching proportion, (b) soluble P leaching proportion, (c) plant enzyme-to-root ratio, (d) microbial enzyme-to-biomass ratio, (e) weathering P flux, and (f) phosphatase activity. In each panel, the case of baseline parameter values is denoted 'BL'. Specific parameter values for each simulation are given in the Supporting Information Notes S1.

When we subjected the +NP treatment to sensitivity analysis, there was little sensitivity of plant biomass to the nutrient-related parameters (Fig. 4). The only exceptions were associated with the most extreme assumptions about plant and microbial enzyme abundances. Therefore, we again found that fertilisation led to an increase in median biomass and a large decrease in biomass range, indicating a stronger control on biomass range from nutrient availability than from the soil texture effects on water availability. Soil-driven variability in PFT abundance persisted in our sensitivity analysis (Figs S4 and S5, Notes S1).

Regional-scale analysis

Our regional-scale analysis characterised the effects of climate on biomass range and PFT composition and was used to test H3. Overall, there was a general tendency to have smaller biomass ranges in the north and larger ranges, up to 80%, in the south (Fig. 5a). Simple linear regression indicated a positive relationship between biomass range and MAP ($R^2 = 0.53$; $P < 0.0001$) (Fig. 5b). However, there was a trend in the residuals ($P = 0.003$): the residuals tended to be positive for low values of MAP and negative for high values of MAP. Provided the outlier point at a MAP of 6875 mm was removed, breakpoint regression (R package 'segmented'; Muggeo (2008)) identified a breakpoint at 1556 mm, with a negative (positive) relationship between MAP and biomass range for MAP smaller (larger) than the breakpoint. In our +NP regional-scale simulation, the biomass ranges were generally smaller, and never larger than 30% (Fig. 5c). The largest ranges emerged in the north of the domain. There was a strictly decreasing linear relationship between MAP and biomass range ($P < 0.0001$) (Fig. 5d), and in this case there was no discernible pattern in the residuals. Low-precipitation grid cells were more sensitive than high-precipitation grid cells to assumptions about soil texture variation (Fig. S6; Notes S1). Although there was regional variability, nitrogen fixation generally reduced variation across OSS (Fig. S7; Notes S1).

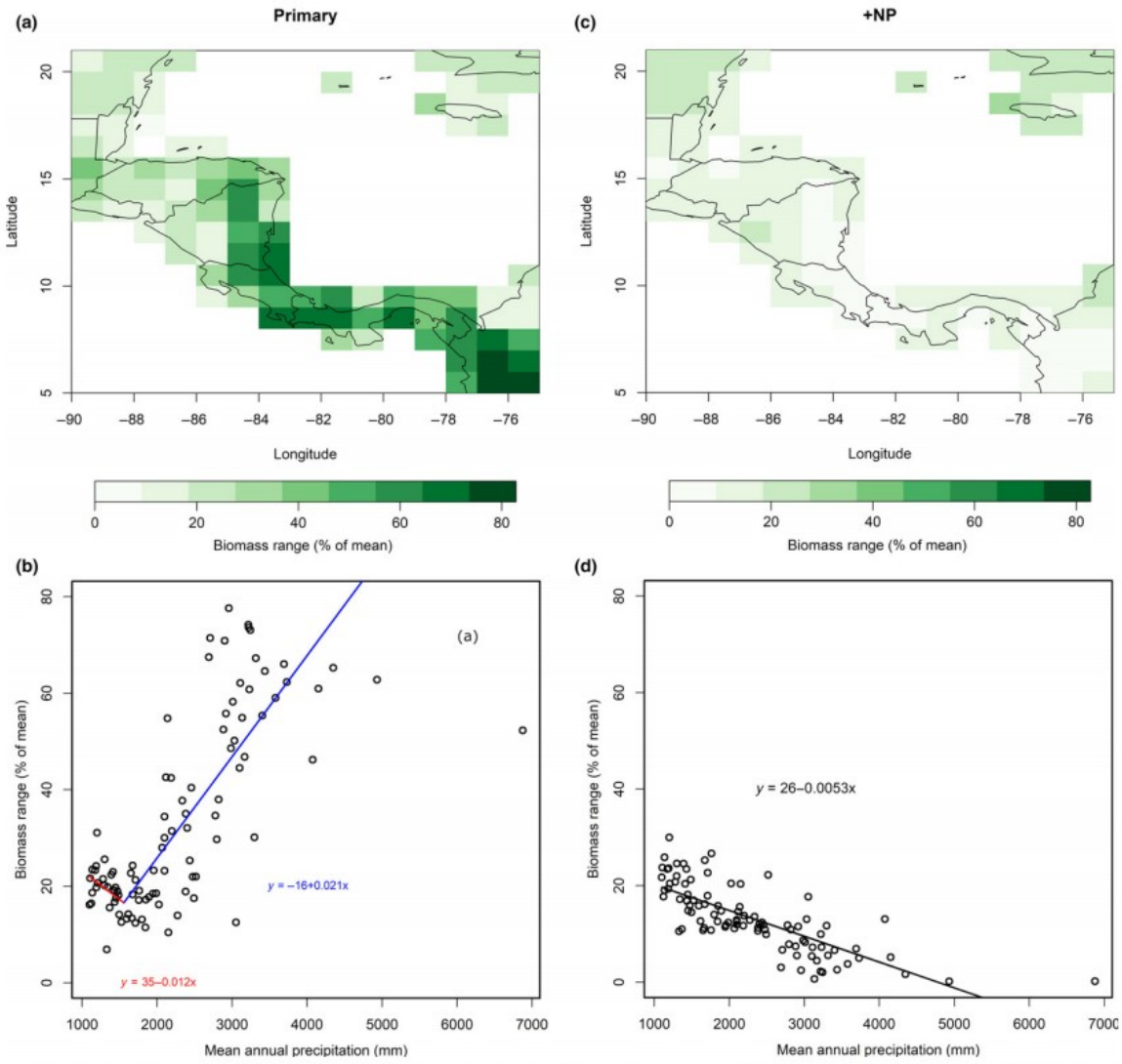

Fig. 5 Regional-scale variation in biomass range across soil substrates. Results from the primary simulation configuration are shown on the left, and results from the fertilised ('+NP') simulation on the right. (a), (c): Spatial distribution of biomass range. (b), (d): Relationship between mean annual precipitation and biomass range for the primary and +NP simulations, respectively. Both simulations used baseline parameter values.

On the regional scale, the entropy index ranged from −1.13 to −0.003 for our primary simulation (Fig. 6a). In nearly all grid cells, fertilisation resulted in less negative entropy values (−0.33 to 0.0) (Fig. 6b), indicating a more random sorting of PFTs across OSS. In both the unfertilised and fertilised cases, the entropy index was uncorrelated with MAP.

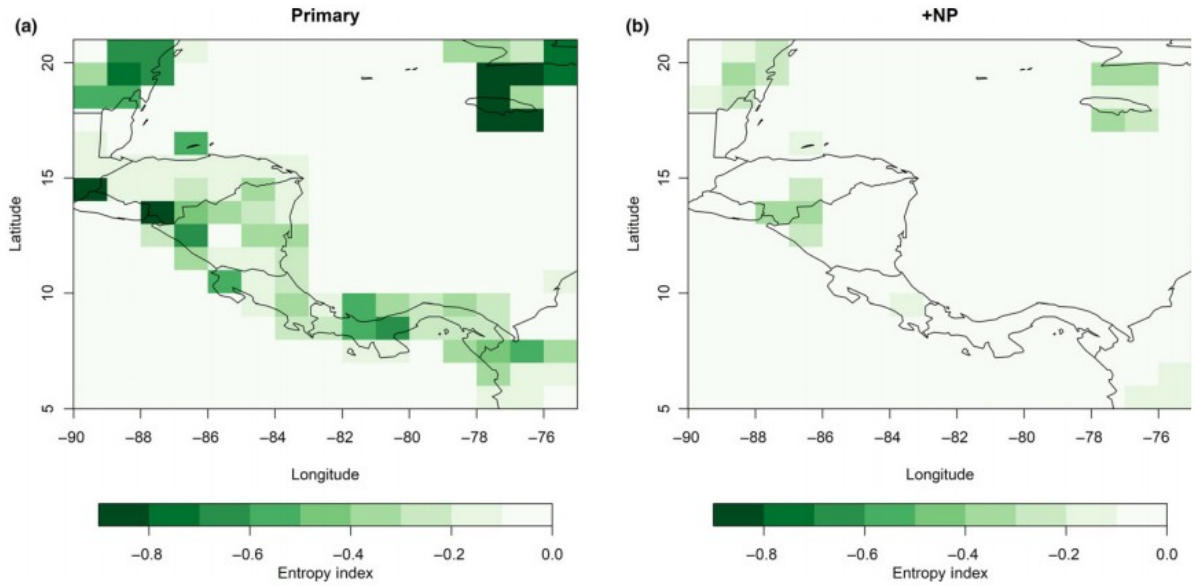

Fig. 6 Regional-scale variability in the entropy index for our primary simulation (a) and for our fertilised ('+NP') simulation (b). The smaller (more negative) the entropy, the more strongly the observed soil state filters plant functional type composition.

Discussion

Model-data comparison

Because we lack initial conditions at the time of agricultural abandonment (Powers *et al*., 2009), it is impossible to configure a simulation to be exactly consistent with field plots. Nevertheless, most of our simulated biomass values were comparable with the observed values (Fig. 1), except for a low bias in the older plots. This bias may be due to errors in the initial conditions (for example reflecting uncertainty in the abundance of remnant trees at the time of abandonment) and/or errors in the simulated growth, mortality, and recruitment rates. We think it unlikely that errors in growth predominate. In a previous analysis, we found that simulated growth rates in nutrient-rich plots compared favourably with observations (Xu *et al*., 2016). Furthermore, our +NP simulation results (Fig. 4) show that, even without nutrient limitation, biomass amounts near the maximum observed values were not simulated. Given the 30 yr timeframe of the simulations, it is unlikely that recruitment errors predominate. Therefore, we regard mortality overestimation to be the most likely cause of the bias.

Plant biomass was related to stand age in observations and simulations, but we found no simple relationship between plant biomass and soil properties. In the observations, this null result may simply be a consequence of random variation. However, it is consistent with previous studies which found that, after stand age, pH (a variable not used in our model) and the traits of the establishing plant community were the best predictors of biomass (Becknell & Powers, 2014), and weak community-level tropical forest P limitation (Turner *et al*., 2018). The relationship between biomass and soil properties is clearly multifaceted, with different factors potentially limiting at different

stand ages or for different plant community composition. For example, N may be limiting earlier in succession (Batterman *et al*., 2013) and P later in succession.

Soil-mediated biomass variation

We evaluated the hypothesis that landscape-scale variation in soil properties would lead to sustained variation in plant biomass in our model simulations (H1). For our grid cell-level simulations of secondary succession in Guanacaste, the biomass range across OSS (Table S1) was *c*. 30% of the mean (Fig. 2). This model result is consistent with several observational tropical forest studies at the landscape and regional scale that have reported a positive correlation between biomass and either soil fertility or clay fraction (Laurance *et al*., 1999; Zarin *et al*., 2001; de Castilho *et al*., 2006; Slik *et al*., 2010). Positive soil fertility effects on biomass have also been observed across landscape gradients (Becknell & Powers, 2014) and fertilisation experiments in TDFs (Campo & Vázquez-Yanes, 2004).

On larger scales, the situation is more complex, in both our simulations and in observations. In accord with H3, we found that the simulated effect of soil properties on biomass range depended on MAP (Fig. 5). Meanwhile, previous observational work found that biomass across Amazonia was been negatively related to soil fertility, and correlated with spatial distributions of plant taxa and traits (Malhi *et al*., 2006; Saatchi *et al*., 2007; Quesada *et al*., 2012). Determining whether our model would capture such observations in Amazonia is beyond the scope of this study, in part because the list of PFTs that we consider here (Table S2) is not representative of Amazonia.

We used a sensitivity analysis to scrutinise our simulation result that a realistic range of OSS can directly lead to a large range in accumulated biomass. Indeed, this result regarding biomass range was nearly independent, both quantitatively and qualitatively, of particular choices for parameter values (Fig. 4). Nevertheless, the average biomass (across OSS) can be very sensitive to parameters. In particular, parameters related to leaching and to specific rates of plant and microbe nutrient acquisition had demonstrably strong effects. These parameters can pertain to both N and P dynamics (Methods S1), and we recognised both of these nutrients as potentially limiting biomass accumulation in TDFs (Campo, 2016; Augusto *et al*., 2017). Future modelling efforts and experiments (and preferably both in concert) should be aimed at improving representations of leaching and plant and microbial nutrient acquisition processes (Notes S2).

While observational studies can assess variation of biomass across OSS, it is more difficult for gradient-based analyses to attribute biomass variation to particular soil properties because more than one soil property usually varies across a gradient (Quesada *et al*., 2012). An advantage of a modelling approach is that it is straightforward to carry out attribution analysis. In particular, we set out to distinguish the hydrological effects of soil texture from the effects of soil fertility. In our +NP simulations, we eliminated plant

nutrient limitation in all but a few cases of parameter values (Fig. 4). Comparing our fertilised and unfertilised grid cell simulations at Guanacaste, we concluded that soil texture variation probably accounted for less than half the range of simulated biomass (Fig. 4).

Soil-mediated variation in ecosystem composition

We found large variation in ecosystem composition, even at the level of presence/absence (H2), across soil types in our primary simulations (Figs. 3a–c, 6a). This result is consistent with observations in Indian TDFs that also identified variation in ecosystem composition with soil texture (Jha & Singh, 1990) and species distribution modelling of Amazonia that strongly correlated species' distributions with a composite 'soil' variable (Figueiredo *et al*., 2018). However, these particular observational analyses did not explicitly control for soil fertility as distinct from soil texture. Werden *et al*. (2018) did address this issue, and found that more species sorted over soil chemistry gradients than soil texture gradients. We built on that analysis through comparison of our primary and +NP simulations. This comparison controls for the hydrological effect of soil texture and, therefore, is able to directly implicate soil fertility as the causal driver for differences in composition in our simulations.

Compositional variation could generally emerge for more than one reason in model simulations. While it could be that soil type strongly filters for particular PFTs, it could also be that different soil types do not filter at all and, therefore, PFTs would establish on different soil types at random. We present here two arguments that PFT composition is filtered by the OSS in our simulations rather than at random. First, our sensitivity analysis showed that PFTs were consistently variable (Fig. S4). For most parameter settings, the standard deviation (across OSS) of the proportion of each PFT was strongly peaked. Such consistency would not be expected if the soils did not filter for particular PFTs and PFTs were therefore randomly distributed. Second, we found that fertilisation strongly increased our entropy index (Figs 6, S5). This result means that PFTs are more randomly distributed across soil types in the +NP simulations than in the primary simulations. Therefore, the primary simulations more strongly filter for PFTs than the fertilised simulations.

In our simulations, different plant strategies and trait values have different degrees of success, depending on soils (Figs. 3a–c, 6; Notes S2). In the Guanacaste grid cell, the biomass was dominated (> 95%) by three PFTs. This level of functional diversity is much less than that observed in nature, but is more than the level of functional diversity exhibited by a traditional dynamic global vegetation model that, by design, only includes one or two tropical tree PFTs and is constrained by climate envelopes (Fisher *et al*., 2015). Our deterministic result therefore presents an interesting complement to other recent models that have replaced the PFT approach to modelling diversity with a trait-based approach in which the traits of individual plants

or cohorts are stochastically assigned and then tracked (Pavlick *et al*., 2013; Scheiter *et al*., 2013; Sakschewski *et al*., 2015). The simulated probabilities of different trait combinations varied across Amazonia and depended largely on climate. We suggest that realistic accounting for geodiversity and allowing for stochastic variation in plant traits are complementary approaches for simulating observed trait distributions.

Soil-mediated variation in other ecosystem properties

In our primary simulations, below-ground resource pools exhibited larger variation across OSS than plant or microbial biomass, GPP, or microbial respiration (Table 1). This result indicates that, in the model, vegetation and microbes can partially compensate for OSS variation. Symbiotic N fixation acted as a compensatory mechanism (Fig. S7), and other likely mechanisms include changes in PFT composition and variable microbial stoichiometry. Compared with the primary simulations, variation in the +NP simulations was smaller for all variables.

From hypothesis testing to prediction

We used a mechanistic model to evaluate hypotheses regarding the effect of soil nutrients and texture on plant biomass accumulation and ecosystem composition. However, models have other uses, including prediction. Further benchmarking is necessary before ED2-MEND-NCOM could be used for that purpose, but we argue that such efforts would be worthwhile in that they could provide a perhaps unique view of nutrient constraints on CO_2 fertilisation, for example. The next steps in this direction should include a comprehensive evaluation of the coupled model against available observations of demographic rates, productivity, composition, as well as below-ground biogeochemical cycling and allocation. In addition, as mentioned above, the PFT list should be expanded so that it is more broadly representative of tropical forests.

Our results pose challenges for Earth system models (ESMs). Because fine-scale geodiversity data are limited, we advocate that modellers and empiricists collaborate to chart a course forward. Given ample observations, OSS could be constructed and an ensemble of ESM simulations could be carried out, with each ensemble member corresponding to an OSS. Grid-scale biomass can be computing by taking an ensemble average. However, bias may be incurred if limited computational resources limit the number of simulations that can be done. In our case study, we found that a single simulation with average soils overestimated biomass, and we expect this result to be general. The reason is that biomass has a non-linear relationship with soil fertility, and eventually saturates at high soil nutrient availability. Evidence for saturation is seen in our +NP simulations: there is very little sensitivity to nutrient-related parameters at high nutrient levels (Fig. 4). Then, because of Jensen's inequality (Ruel & Ayres, 1999), an ensemble of simulations that fully captures soil variation would have a smaller average biomass than a single simulation initialised with an average OSS.

Our simulations demonstrate that variation in soils can be mechanistically linked to variation in plant biomass and PFT composition. A more sophisticated representation of geodiversity in models would therefore be likely to improve simulations and enhance understanding of vegetation functioning and composition. While further steps are needed to better resolve variation in nutrient cycles, the effects of geomorphological variation and subgrid hydrological interconnectivity (Balvanera *et al*., 2011; Jucker *et al*., 2018; Schwantes *et al*., 2018) should also be considered within an overarching framework. Going forward, determining such impacts of geodiversity across tropical ecosystems should be a high-priority research goal.

Acknowledgements

DM, BGW, and JSP were supported by the US Department of Energy, Office of Science, Terrestrial Ecosystem Science Program, Award DE-SC0014363. The field plots were maintained by National Science Foundation CAREER Grant DEB-1053237 to JSP. GW was supported by the Energy Exascale Earth System Model (E3SM) project and the Climate Model Development & Validation (CMDV) project under contract DE-AC05-00OR22725 to Oak Ridge National Laboratory. WJR and QZ were supported by the RUBISCO Scientific Focus Area under contract DE-AC02-05CH11231 to Lawrence Berkeley National Laboratory. The original manuscript was significantly improved by the comments of four anonymous reviewers.

References

Allison SD, Wallenstein MD, Bradford MA. 2010. Soil-carbon response to warming dependent on microbial physiology. *Nature Geoscience* 3: 336– 340.

Augusto L, Achat DL, Jonard M, Vidal D, Ringeval B. 2017. Soil parent material—A major driver of plant nutrient limitations in terrestrial ecosystems. *Global Change Biology* 23: 3808– 3824.

Avitabile V, Herold M, Heuvelink GB, Lewis SL, Phillips OL, Asner GP, Armston J, Ashton PS, Banin L, Bayol N *et al*. 2016. An integrated pan-tropical biomass map using multiple reference datasets. *Global Change Biology* 22: 1406– 1420.

Balvanera P, Quijas S, Perez-Jimenez A. 2011. Distribution patterns of tropical dry forest trees along a mesoscale water availability gradient. *Biotropica* 43: 414– 422.

Batterman SA, Hedin LO, Van Breugel M, Ransijn J, Craven DJ, Hall JS. 2013. Key role of symbiotic dinitrogen fixation in tropical forest secondary succession. *Nature* 502: 224– 227.

Becknell JM, Kissing LB, Powers JS. 2012. Aboveground biomass in mature and secondary seasonally dry tropical forests: a literature review and global synthesis. *Forest Ecology and Management* 276: 88– 95.

Becknell JM, Powers JS. 2014. Stand age and soils as drivers of plant functional traits and aboveground biomass in secondary tropical dry forest. *Canadian Journal of Forest Research* 44: 604– 613.

Beer C, Reichstein M, Tomelleri E, Ciais P, Jung M, Carvalhais N, Rodenbeck C, Arain MA, Baldocchi D, Bonan GB *et al*. 2010. Terrestrial gross carbon dioxide uptake: global distribution and covariation with climate. *Science* 329: 834– 838.

Binkley D, Giardina C. 1998. Why do tree species affect soils? The warp and woof of tree-soil interactions. *Biogeochemistry* 42: 89– 106.

Calvo-Alvarado J, McLennan B, Sánchez-Azofeifa A, Garvin T. 2009. Deforestation and forest restoration in Guanacaste, Costa Rica: putting conservation policies in context. *Forest Ecology and Management* 258: 931– 940.

Camenzind T, Hättenschwiler S, Treseder KK, Lehmann A, Rillig MC. 2018. Nutrient limitation of soil microbial processes in tropical forests. *Ecological Monographs* 88: 4– 21.

Campo J. 2016. Shift from ecosystem P to N limitation at precipitation gradient in tropical dry forests at Yucatan, Mexico. *Environmental Research Letters* 11: 095006.

Campo J, Vázquez-Yanes C. 2004. Effects of nutrient limitation on aboveground carbon dynamics during tropical dry forest regeneration in Yucatán, Mexico. *Ecosystems* 7: 311– 319.

de Castilho CV, Magnusson WE, de Araújo RNO, Luizao RC, Luizao FJ, Lima AP, Higuchi N. 2006. Variation in aboveground tree live biomass in a central Amazonian Forest: effects of soil and topography. *Forest Ecology and Management* 234: 85– 96.

Clark DB, Clark DA, Read JM. 1998. Edaphic variation and the mesoscale distribution of tree species in a neotropical rain forest. *Journal of Ecology* 86: 101– 112.

Cleveland CC, Townsend AR, Taylor P, Alvarez-Clare S, Bustamante MMC, Chuyong G, Dobrowski SZ, Grierson P, Harms KE, Houlton BZ *et al*. 2011. Relationships among net primary productivity, nutrients and climate in tropical rain forest: a pan-tropical analysis. *Ecology Letters* 14: 939– 947.

Condit R, Engelbrecht BM, Pino D, Pérez R, Turner BL. 2013. Species distributions in response to individual soil nutrients and seasonal drought across a community of tropical trees. *Proceedings of the National Academy of Sciences, USA* 110: 5064– 5068.

Fayolle A, Engelbrecht B, Freycon V, Mortier F, Swaine M, Réjou-Méchain M, Doucet J-L, Fauvet N, Cornu G, Gourlet-Fleury S. 2012. Geological substrates shape tree species and trait distributions in African moist forests. *PLoS ONE* 7: e42381.

Figueiredo FOG, Zuquim G, Tuomisto H, Moulatlet GM, Balslev H, Costa FRC. 2018. Beyond climate control on species range: the importance of soil data to predict distribution of Amazonian plant species. *Journal of Biogeography* 45: 190– 200.

Fisher R, Muszala S, Verteinstein M, Lawrence P, Xu C, McDowell N, Knox R, Koven C, Holm J, Rogers B *et al*. 2015. Taking off the training wheels: the properties of a dynamic vegetation model without climate envelopes. *Geoscientific Model Development Discussions* 8: 3593– 3619.

Fujii K, Shibata M, Kitajima K, Ichie T, Kitayama K, Turner BL. 2017. Plant–soil interactions maintain biodiversity and functions of tropical forest ecosystems. *Ecological Research* 33: 49– 160.

Gei M, Rozendaal DM, Poorter L, Bongers F, Sprent JI, Garner MD, Aide TM, Andrade JL, Balvanera P, Becknell JM *et al*. 2018. Legume abundance along successional and rainfall gradients in Neotropical forests. *Nature Ecology & Evolution* 2: 1104– 1111.

Georgiou K, Abramoff RZ, Harte J, Riley WJ, Torn MS. 2017. Microbial community-level regulation explains soil carbon responses to long-term litter manipulations. *Nature Communications* 8: 1223.

Gerber S, Hedin LO, Oppenheimer M, Pacala SW, Shevliakova E. 2010. Nitrogen cycling and feedbacks in a global dynamic land model. *Global Biogeochemical Cycles* 24: GB1001.

Goll DS, Brovkin V, Parida B, Reick CH, Kattge J, Reich PB, Van Bodegom P, Niinemets Ü. 2012. Nutrient limitation reduces land carbon uptake in simulations with a model of combined carbon, nitrogen and phosphorus cycling. *Biogeosciences* 9: 3547– 3569.

Gray M. 2008. Geodiversity: developing the paradigm. *Proceedings of the Geologists' Association* 119: 287– 298.

Gutschick V. 1981. Evolved strategies in nitrogen acquisition by plants. *American Naturalist* 118: 607– 637.

Hartshorn GS. 1983. Plants. In: DH Janzen, ed. *Costa Rican Natural History*. Chicago, IL, USA: University of Chicago Press, 118– 157.

Holdridge LR. 1947. Determination of world plant formations from simple climatic data. *Science* 105: 367– 368.

Jenny H. 1941. *Factors of soil formation: a system of quantitative pedology*. Mineola, NY, USA: Dover.

Jha C, Singh JS. 1990. Composition and dynamics of dry tropical forest in relation to soil texture. *Journal of Vegetation Science* 1: 609– 614.

John R, Dalling JW, Harms KE, Yavitt JB, Stallard RF, Mirabello M, Hubbell SP, Valencia R, Navarrete H, Vallejo M *et al*. 2007. Soil nutrients influence spatial

distributions of tropical tree species. *Proceedings of the National Academy of Sciences, USA* 104: 864– 869.

Jubanski J, Ballhorn U, Kronseder K, Franke J, Siegert F. 2013. Detection of large above-ground biomass variability in lowland forest ecosystems by airborne LiDAR. *Biogeosciences* 10: 3917– 3930.

Jucker T, Bongalov B, Burslem D, Nilus R, Dalponte M, Lewis SL, Phillips OL, Qie L, Coomes DA. 2018. Topography shapes the structure, composition and function of tropical forest landscapes. *Ecology Letters* 21: 989– 1000.

Laurance WF, Fearnside PM, Laurance SG, Delamonica P, Lovejoy TE, Rankin-de Merona JM, Chambers JQ, Gascon C. 1999. Relationship between soils and Amazon forest biomass: a landscape-scale study. *Forest Ecology and Management* 118: 127– 138.

Leiva JA, Mata R, Rocha OJ, Gutiérrez Soto MV. 2009. Cronología de la regeneración del bosque tropical seco en Santa Rosa, Guanacaste, Costa Rica: I. Características edáficas. *Revista de Biología Tropical* 57: 801– 815.

Levine NM, Zhang K, Longo M, Baccini A, Phillips OL, Lewis SL, Alvarez-Dávila E, de Andrade ACS, Brienen RJ, Erwin TL *et al*. 2016. Ecosystem heterogeneity determines the ecological resilience of the Amazon to climate change. *Proceedings of the National Academy of Sciences, USA* 113: 793–797.

Levy P, Cannell M, Friend A. 2004. Modelling the impact of future changes in climate, CO_2 concentration and land use on natural ecosystems and the terrestrial carbon sink. *Global Environmental Change* 14: 21– 30.

Longo M, Knox RG, Levine NM, Alves LF, Bonal D, Camargo PB, Fitzjarrald DR, Hayek MN, Restrepo-Coupe N, Saleska SR *et al*. 2018. Ecosystem heterogeneity and diversity mitigate Amazon forest resilience to frequent extreme droughts. *New Phytologist* 219: 914– 931.

Malhi Y, Wood D, Baker TR, Wright J, Phillips OL, Cochrane T, Meir P, Chave J, Almeida S, Arroyo L *et al*. 2006. The regional variation of aboveground live biomass in old-growth Amazonian forests. *Global Change Biology* 12: 1107–1138.

Medvigy D, Wofsy S, Munger J, Hollinger D, Moorcroft P. 2009. Mechanistic scaling of ecosystem function and dynamics in space and time: Ecosystem Demography model version 2. *Journal of Geophysical Research: Biogeosciences* 114: G01002.

Miles L, Newton AC, DeFries RS, Ravilious C, May I, Blyth S, Kapos V, Gordon JE. 2006. A global overview of the conservation status of tropical dry forests. *Journal of Biogeography* 33: 491– 505.

Moorcroft PR, Hurtt G, Pacala SW. 2001. A method for scaling vegetation dynamics: the ecosystem demography model (ED). *Ecological Monographs* 71: 557– 586.

Muggeo VM. 2008. Segmented: an R package to fit regression models with broken-line relationships. *R News* 8: 20– 25.

Murphy JM, Sexton DM, Barnett DN, Jones GS, Webb MJ, Collins M, Stainforth DA. 2004. Quantification of modelling uncertainties in a large ensemble of climate change simulations. *Nature* 430: 768– 772.

O'Brien MJ, Peréz-Aviles D, Powers JS. 2018. Resilience of seed production to a severe El Niño-induced drought across functional groups and dispersal types. *Global Change Biology* 24: 5270– 5280.

Pappas C, Fatichi S, Rimkus S, Burlando P, Huber MO. 2015. The role of local-scale heterogeneities in terrestrial ecosystem modeling. *Journal of Geophysical Research: Biogeosciences* 120: 341– 360.

Pavlick R, Drewry DT, Bohn K, Reu B, Kleidon A. 2013. The Jena Diversity-Dynamic Global Vegetation Model (JeDi-DGVM): a diverse approach to representing terrestrial biogeography and biogeochemistry based on plant functional trade-offs. *Biogeosciences* 10: 4137– 4177.

Poorter L, Bongers F, Aide TM, Zambrano AMA, Balvanera P, Becknell JM, Boukili V, Brancalion PH, Broadbent EN, Chazdon RL *et al*. 2016. Biomass resilience of Neotropical secondary forests. *Nature* 530: 211– 214.

Powers JS, Becknell JM, Irving J, Perez-Aviles D. 2009. Diversity and structure of regenerating tropical dry forests in Costa Rica: geographic patterns and environmental drivers. *Forest Ecology and Management* 258: 959– 970.

Powers JS, Perez-Aviles D. 2013. Edaphic factors are a more important control on surface fine roots than stand age in secondary tropical dry forests. *Biotropica* 45: 1– 9.

Quesada C, Phillips O, Schwarz M, Czimczik C, Baker T, Patiño S, Fyllas N, Hodnett M, Herrera R, Almeida S *et al*. 2012. Basin-wide variations in Amazon forest structure and function are mediated by both soils and climate. *Biogeosciences* 9: 2203– 2246.

Reed SC, Yang X, Thornton PE. 2015. Incorporating phosphorus cycling into global modeling efforts: a worthwhile, tractable endeavor. *New Phytologist* 208: 324– 329.

Ruban DA. 2010. Quantification of geodiversity and its loss. *Proceedings of the Geologists' Association* 121: 326– 333.

Ruel JJ, Ayres MP. 1999. Jensen's inequality predicts effects of environmental variation. *Trends in Ecology & Evolution* 14: 361– 366.

Saatchi SS, Houghton R, Dos Santos Alvala R, Soares JV, Yu Y. 2007. Distribution of aboveground live biomass in the Amazon basin. *Global Change Biology* 13: 816– 837.

Sakschewski B, Bloh W, Boit A, Rammig A, Kattge J, Poorter L, Peñuelas J, Thonicke K. 2015. Leaf and stem economics spectra drive diversity of

functional plant traits in a dynamic global vegetation model. *Global Change Biology* 21: 2711– 2725.

Scheiter S, Langan L, Higgins SI. 2013. Next-generation dynamic global vegetation models: learning from community ecology. *New Phytologist* 198: 957– 969.

Schwantes AM, Parolari AJ, Swenson JJ, Johnson DM, Domec JC, Jackson RB, Pelak N, Porporato A. 2018. Accounting for landscape heterogeneity improves spatial predictions of tree vulnerability to drought. *New Phytologist* 220: 132– 146.

Sheffield J, Goteti G, Wood EF. 2006. Development of a 50-year high-resolution global dataset of meteorological forcings for land surface modeling. *Journal of Climate* 19: 3088– 3111.

Sitch S, Friedlingstein P, Gruber N, Jones S, Murray-Tortarolo G, Ahlström A, Doney SC, Graven H, Heinze C, Huntingford C *et al*. 2015. Recent trends and drivers of regional sources and sinks of carbon dioxide. *Biogeosciences* 12: 653– 679.

Sitch S, Smith B, Prentice IC, Arneth A, Bondeau A, Cramer W, Kaplan J, Levis S, Lucht W, Sykes MT *et al*. 2003. Evaluation of ecosystem dynamics, plant geography and terrestrial carbon cycling in the LPJ dynamic global vegetation model. *Global Change Biology* 9: 161– 185.

Slik J, Aiba SI, Brearley FQ, Cannon CH, Forshed O, Kitayama K, Nagamasu H, Nilus R, Payne J, Paoli G *et al*. 2010. Environmental correlates of tree biomass, basal area, wood specific gravity and stem density gradients in Borneo's tropical forests. *Global Ecology and Biogeography* 19: 50– 60.

Soil Survey Staff. 1999. *Soil taxonomy, a basic system of soil classification for making and interpreting soil surveys*. Washington, DC, USA: United States Department of Agriculture, Natural Resources Conservation Service.

Tang J, Riley W. 2013. A total quasi-steady-state formulation of substrate uptake kinetics in complex networks and an example application to microbial litter decomposition. *Biogeosciences* 10: 8329– 8351.

Tang J, Riley WJ. 2015. Weaker soil carbon–climate feedbacks resulting from microbial and abiotic interactions. *Nature Climate Change* 5: 56– 60.

Thornton PE, Lamarque JF, Rosenbloom NA, Mahowald NM. 2007. Influence of carbon-nitrogen cycle coupling on land model response to CO_2 fertilization and climate variability. *Global Biogeochemical Cycles* 21: GB4018.

Thornton PE, Rosenbloom NA. 2005. Ecosystem model spin-up: estimating steady state conditions in a coupled terrestrial carbon and nitrogen cycle model. *Ecological Modelling* 189: 25– 48.

Townsend AR, Asner GP, Cleveland CC. 2008. The biogeochemical heterogeneity of tropical forests. *Trends in Ecology & Evolution* 23: 424– 431.

Turner BL, Brenes-Arguedas T, Condit R. 2018. Pervasive phosphorus limitation of tree species but not communities in tropical forests. *Nature* 555: 367– 370.

Wang G, Huang W, Mayes MA, Liu X, Zhang D, Zhang Q, Han T, Zhou G. 2019. Soil moisture drives microbial controls on carbon decomposition in two subtropical forests. *Soil Biology and Biochemistry* 130: 185– 194.

Wang G, Jagadamma S, Mayes MA, Schadt CW, Steinweg JM, Gu L, Post WM. 2015a. Microbial dormancy improves development and experimental validation of ecosystem model. *ISME Journal* 9: 226– 237.

Wang K, Peng C, Zhu Q, Zhou X, Wang M, Zhang K, Wang G. 2017. Modeling global soil carbon and soil microbial carbon by integrating microbial processes into the ecosystem process model TRIPLEX-GHG. *Journal of Advances in Modeling Earth Systems* 9: 2368– 2384.

Wang G, Post WM, Mayes MA. 2013. Development of microbial-enzyme-mediated decomposition model parameters through steady-state and dynamic analyses. *Ecological Applications* 23: 255– 272.

Wang Y-P, Zhang Q, Pitman AJ, Dai Y. 2015b. Nitrogen and phosphorous limitation reduces the effects of land use change on land carbon uptake or emission. *Environmental Research Letters* 10: 014001.

Waring BG, Álvarez-Cansino L, Barry KE, Becklund KK, Dale S, Gei MG, Keller AB, Lopez OR, Markesteijn L, Mangan S *et al*. 2015a. Pervasive and strong effects of plants on soil chemistry: a meta-analysis of individual plant ‘Zinke'effects. *Proceedings of the Royal Society of London. Series B, Biological Sciences* 282: 20151001.

Waring BG, Aviles DP, Murray J, Powers J. in press. Plant community responses to stand-level nutrient fertilization in a secondary tropical dry forest. *Ecology*. doi: 10.1002/ecy.2691.

Waring BG, Becknell JM, Powers JS. 2015b. Nitrogen, phosphorus, and cation use efficiency in stands of regenerating tropical dry forest. *Oecologia* 178: 887– 897.

Waring BG, Gei MG, Rosenthal L, Powers JS. 2016. Plant–microbe interactions along a gradient of soil fertility in tropical dry forest. *Journal of Tropical Ecology* 32: 314– 323.

Werden LK, Becknell JM, Powers JS. 2018. Edaphic factors, successional status and functional traits drive habitat associations of trees in naturally regenerating tropical dry forests. *Functional Ecology* 32: 2766– 2776.

Wieder WR, Allison SD, Davidson EA, Georgiou K, Hararuk O, He Y, Hopkins F, Luo Y, Smith MJ, Sulman B *et al*. 2015. Explicitly representing soil microbial processes in Earth system models. *Global Biogeochemical Cycles* 29: 1782– 1800.

Wright SJ, Yavitt JB, Wurzburger N, Turner BL, Tanner EV, Sayer EJ, Santiago LS, Kaspari M, Hedin LO, Harms KE *et al*. 2011. Potassium, phosphorus, or nitrogen limit root allocation, tree growth, or litter production in a lowland tropical forest. *Ecology* 92: 1616– 1625.

Xu X, Medvigy D, Powers JS, Becknell JM, Guan K. 2016. Diversity in plant hydraulic traits explains seasonal and inter-annual variations of vegetation dynamics in seasonally dry tropical forests. *New Phytologist* 212: 80– 95.

Yang X, Thornton P, Ricciuto D, Post W. 2014. The role of phosphorus dynamics in tropical forests. *Biogeosciences* 11: 1667– 1681.

Zarin DJ, Ducey MJ, Tucker JM, Salas WA. 2001. Potential biomass accumulation in Amazonian regrowth forests. *Ecosystems* 4: 658– 668.

Zhu Q, Riley WJ, Tang J. 2017. A new theory of plant–microbe nutrient competition resolves inconsistencies between observations and model predictions. *Ecological Applications* 27: 875– 886.

Zhu Q, Riley W, Tang J, Koven C. 2016. Multiple soil nutrient competition between plants, microbes, and mineral surfaces: model development, parameterization, and example applications in several tropical forests. *Biogeosciences* 13: 341– 363.